Journal of Anatomy

J. Anat. (2016) **228**, pp996–1005 doi: 10.1111/joa.12448

Stereological assessment of sexual dimorphism in the rat liver reveals differences in hepatocytes and Kupffer cells but not hepatic stellate cells

Ricardo Marcos,[1,2] Célia Lopes,[1,2] Fernanda Malhão,[1,2] Carla Correia-Gomes,[3] Sónia Fonseca,[4] Margarida Lima,[4] Rolf Gebhardt[5] and Eduardo Rocha[1,2]

[1]*Laboratory of Histology and Embryology, Department of Microscopy, ICBAS – Institute of Biomedical Sciences Abel Salazar, U.Porto – University of Porto, Porto, Portugal*
[2]*Histomorphology, Physiopathology and Applied Toxicology Group, CIIMAR – Interdisciplinary Centre of Marine and Environmental Research, U.Porto – University of Porto, Porto, Portugal*
[3]*Scotland's Rural College, Epidemiology Research Unit – Future Farming Systems Group, Inverness, UK*
[4]*Laboratory of Cytometry, Department of Hematology, UMIB – Unit for Multidisciplinary Research in Biomedicine, CHP – Centro Hospitalar do Porto, ICBAS – Institute of Biomedical Sciences Abel Salazar, HSA – Hospital de Santo António, U.Porto – University of Porto, Porto, Portugal*
[5]*Institute of Biochemistry, Faculty of Medicine, University of Leipzig, Leipzig, Germany*

Abstract

There is long-standing evidence that male and female rat livers differ in enzyme activity. More recently, differences in gene expression profiling have also been found to exist; however, it is still unclear whether there is morphological expression of male/female differences in the normal liver. Such differences could help to explain features seen at the pathological level, such as the greater regenerative potential generally attributed to the female liver. In this paper, hepatocytes (HEP), Kupffer cells (KC) and hepatic stellate cells (HSC) of male and female rats were examined to investigate hypothesised differences in number, volume and spatial co-localisation of these cell types. Immunohistochemistry and design-based stereology were used to estimate total numbers, numbers per gram and mean cell volumes. The position of HSC within lobules (periportal vs. centrilobular) and their spatial proximity to KC was also assessed. In addition, flow cytometry was used to investigate the liver ploidy. In the case of HEP and KC, differences in the measured cell parameters were observed between male and female specimens; however, no such differences were detected for HSC. Female samples contained a higher number of HEP per gram, with more binucleate cells. The HEP nuclei were smaller in females, which was coincident with more abundant diploid particles in these animals. The female liver also had a greater number of KC per gram, with a lower percentage of KC in the vicinity of HSC compared with males. In this study, we document hitherto unknown morphological sexual dimorphism in the rat liver, namely in HEP and KC. These differences may account for the higher regenerative potential of the female liver and lend weight to the argument for considering the rat liver as a sexually dimorphic organ.

Key words: dimorphism; hepatic stellate cells; hepatocytes; Kupffer cells; liver; stereology.

Introduction

Biological inequality is related to so-called gender or sexual dimorphism, in which females have an increased resistance to premature ageing, nutrient deprivation, vascular and heart diseases, brain disorders, as well as hepatic neoplasms and hepatitis C virus infection (Li et al. 2012; Grebely et al. 2014). Evidence has mounted over the past 30 years that the mammalian liver is responsive to steroid sex hormones. These can modulate many functional features of the organ; apart from the differences in cytochrome-P-450, diverse contents of glucose-6-phosphatase (Teutsch, 1984), glutamine synthetase (Sirma et al. 1996) and lipogenic enzymes (Scheicher et al. 2015) have been reported. Pathological features are also modulated by sex hormones, illustrated by the fact that progression to cirrhosis in men can occur at a rate 10 times faster than that seen in women

Correspondence
Ricardo Marcos, Laboratory of Histology and Embryology, Institute of Biomedical Sciences Abel Salazar, Rua de Jorge Viterbo Ferreira no. 228, 4050-313 Porto, Portugal. E: rmarcos@icbas.up.pt

Accepted for publication *5 January 2016*
Article published online *19 February 2016*

(Poynard et al. 2001; Massard et al. 2006; Villa, 2008). *In vitro* studies showed that oestrogens have antioxidant properties, reducing proliferation and collagen synthesis in cultured hepatic stellate cells (HSC; Yasuda et al. 1999). There is no doubt that, at first sight, the microscopic morphology of the liver appears similar in both sexes; however, it is unknown whether male and female HSC differ in volume, number, surrounding cells or position within the liver lobules. As HSC are strongly influenced by the surrounding milieu (Kmieć, 2001), such differences would explain, at least partially, the faster progression of collagen deposition in males.

The liver also exhibits sexual dimorphism in its capacity to regenerate. Unlike most organs, the liver can increase its cell numbers after injury, restoring the lost mass to obtain its optimal volume. Experimental studies in rats have shown a higher degree of regeneration in females (Tsukamoto & Kojo, 1990; Biondo-Simões et al. 2006; Kitagawa et al. 2009) and the scarce clinical data in humans also points in the same direction (e.g. Imamura et al. 1999). Liver regeneration is of utmost importance in liver transplantation, namely when 'small for size' grafts are used. Among the many proliferation factors, the 'augmenter of liver regeneration' is an enigmatic protein released by hepatocytes (HEP) that promotes liver growth (Biondo-Simões et al. 2006; Gandhi, 2012). Recently, it was shown that hepatocellular proliferation depends on the integrity of the Kupffer cells (KC), as their depletion with gadolinium chloride significantly reduced the increase in organ weight, as well as survival after small-for-size transplantation among a cohort of rats (Yang et al. 2013). Still, studies of the ratio of KC to HEP remain scarce (Santos et al. 2009), and it remains unknown whether this ratio differs between the sexes. Intersexual differences in HEP and KC could help to explain the increased risk of graft loss in female-to-male liver transplants (Lai et al. 2011; Croome et al. 2014).

A potential mechanism behind the dimorphic liver regeneration is related to ploidy differences, as diploid HEP are known to divide more rapidly than polyploid cells after hepatectomy (Gupta, 2000). Cell ploidy is classically related to the cell volume (Epstein, 1967), but male vs. female differences in this parameter have never been detailed by morphometry or stereology. Nevertheless, it would be interesting to relate such data to DNA staining with propidium iodide and flow cytometry, which are well recognised tools to evaluate ploidy, based on cell DNA content (Gupta, 2000).

In view of the state of the art, we hypothesised that there are structural differences in the normal liver of males and females that could help explain differences in pathological scenarios. To help elucidate the hypothesis, we combined design-based stereology and flow cytometry to disclose sexual dimorphism in selected targets cells of the rat liver. We first checked whether significant differences existed in collagen in the lobules, the main endpoint of HSC activity. Apart from evaluating the total number and number per gram, we looked at the volume and intralobular position of these cells. As it is recognised that the first fibrogenic stimulus is modulated by KC, we not only estimated their total number and number per gram but also quantified their proximity to HSC. Moreover, we examined the numbers and percentage of binucleate hepatocytes (BnHEP), as well as their cell and nuclear volume. The latter data enabled us to better evaluate, by a morphological approach, whether differences in ploidy existed across males and females. These were later evaluated by a flow cytometry approach.

Materials and methods

Animals

We used male and female Wistar rats ($n = 5$ per group) aged 2 months old, bought from Charles River Laboratories (Barcelona, Spain). All animals had been weaned at 20 days and kept in standard conditions, receiving water and food *ad libitum* in a controlled environment (temperature of 25 °C and 12 h alternated light–dark cycles, with light period starting at 07.00 hours). Males weighed 351 ± 17 g and females 216 ± 13 g. The management of animals and procedures followed the European Union Directives (1999/575/CE and 2010/63/UE) for the protection of animals used for scientific purposes.

Tissue preparation

Sampling was performed during the morning period (from 10.00 to 12.00 hours), to circumvent oscillations in liver functions due to circadian rhythmicity (Davidson et al. 2004). In females, daily vaginal cytologies were observed, to avoid collecting samples in proestrous/oestrous days. Beforehand, animals were deeply anaesthetised with ketamine plus xylazine and blood was collected from the heart and centrifuged to obtain serum for assessing alanine and aspartate transaminase levels. Transcardiac perfusion was performed for 15 min with an isosmotic solution, the liver was weighed and its volume determined by the Scherle's method, as detailed elsewhere (Marcos et al. 2012). A smooth fractionator sampling scheme was applied: half of the paraffin blocks were used for thick sections (30 μm thick) and exhaustively sectioned in a motorised microtome, and the other half were used for thin sections (3 μm thick) (Fig. 1). In thick sections, we sampled five sections of every 30, which were immunostained against: (1) glial fibrillary acidic protein for estimating the total number and number per gram of HSC; (2) ED2 for estimating these parameters in KC; (3) E-cadherin, to differentiate mononucleated from BnHEP, estimating their percentage, and assessing the total number and number per gram of HEP; (4) glial fibrillary acidic protein and glutamine synthetase (an established marker of centrilobular HEP; Gebhardt & Mecke, 1983), to evaluate the lobular distribution of HSC; (5) glial fibrillary acidic protein and ED2 to study the proximity between HSC and KC. The thin sections were used for immunohistochemistry against glial fibrillary acidic protein, to determine the relative volume of HSC (Fig. 2), and for histochemical staining with Sirius red, to assess the relative volume of fibrous tissue.

Thick sections

Immunohistochemistry

The protocol used for thick sections has been described previously (Marcos et al. 2004, 2006). Briefly, antigen recovery was carried out in a microwave (4 + 4 min, at 600 W) and a streptavidin-biotin protocol was used (Histostain Plus, Invitrogen, Camarillo, CA, USA). For glial fibrillary acidic protein, we used 1 : 3000 rabbit polyclonal antibody (Dako, Glostrup, Denmark). For ED2 and E-cadherin we used monoclonal mouse antibodies from Serotec (UK) diluted at 1 : 100 and from Dako (clone NCH 38) diluted at 1 : 250. All slides were incubated for 4 days at 4 °C.

Slides for double immunohistochemistry were also placed in the microwave (this time for three cycles of 4 min). After blocking endogenous biotin and peroxidase, the first streptavidin-biotin protocol was followed, with antibody against glial fibrillary acidic protein (1 : 1500 dilution for 4 days at 4 °C). Slides were developed for 2 min in 0.05% 3,3′-diaminobenzidine (Dako) in Tris-buffered saline with 0.03% H_2O_2 and were then rinsed in tap-water and dipped in 50 mM glycine buffer (pH 2.2) for 5 min, to strip off the antibodies of the first immunoreaction. The second streptavidin-biotin protocol followed, using 1 : 4000 rabbit polyclonal antibody against glutamine synthetase (kind gift of Professor Rolf Gebhardt, University of Leipzig), for another 4 days at 4 °C. Slides were developed with aminoethylcarbazole (Dako) for 10–20 min (the final red colour was controlled by microscopic observation) and slides were mounted in Aquatex (Dako). Regarding the use of double immunohistochemistry to evaluate the proximity of HSC and KC, the protocol was similar to that described above, except for the second antibody (ED2 at 1 : 100 dilution).

Stereological analysis

We used a stereology workstation detailed elsewhere (Marcos et al. 2004) with Olympus CAST-Grid software (version 1.5; Olympus). At the monitor, a final magnification of 4750× allowed an easy and accurate recognition of all cells. Throughout the disector height (20 μm), a software-generated counting frame was superimposed with defined areas (1673, 1267 and 418 μm^2 for HSC, KC and HEP, respectively). In the slides used for assessing the position of HSC within the lobule, a systematic uniform random sampling was also used, but HSC were counted only if fields were in the vicinity of the portal tracts or central venules (we settled these areas as five to six HEP around these landmarks). For the double immunohistochemistry of HSC and KC, the largest counting grid was used and a minimum of 100 HSC were evaluated per animal (Fig. 3).

For counting cells, the nucleus was selected as the counting unit (in the case of BnHEP, this was predetermined to be the first nucleus appearing in focus). Cells were counted following the optical disector rules (Marcos et al. 2004, 2006). The potential bias from lost caps was avoided by having upper and lower guard heights,

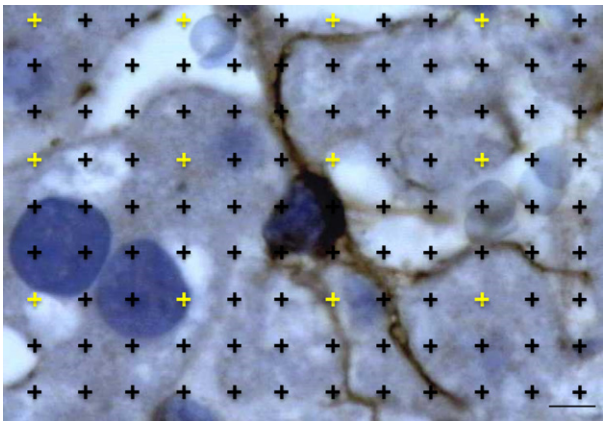

Figure 2 Thin liver section immune-stained against glial fibrillary acidic protein for detecting hepatic stellate cells (HSC). The relative volume of HSC was estimated by counting points falling within HSC and within the reference space (whole liver). To avoid counting an excessive number of points, two different point densities were used: the sparser points (in yellow) quantified the whole liver. Scale bar: 4 μm.

which previously have been validated for the rat liver (Marcos et al. 2012). The collapse in the *z*-direction was also evaluated, by measuring the full section thickness with the microcator in every fifth field (Dorph-Petersen et al. 2001).

The total number of HSC, KC and HEP in the whole liver was primarily estimated according to the optical fractionator rules, meaning that the inverse of block, section, area and height sampling fraction were multiplied by the number of cells counted in the disectors (Marcos et al. 2012). Simultaneously, the number per gram was determined, as this can aid when comparing values between animals with different liver weights. The coefficient of error of the number of cells counted was estimated, using formulae described elsewhere (Marcos et al. 2004).

Additionally, the number-weighted mean cell and nuclear volume of mononuclear and BnHEP was estimated by the nucleator method (Gundersen, 1988; Marcos et al. 2012). In this case, HEP were first sampled by the optical disector and their nucleoli selected. Afterwards, the software generated two isotropic lines from the nucleolus and the intersections between these lines, and nuclear and cell borders were marked. The average distance from the intersections to the nucleolus was used to estimate the number-weighted mean cell and nuclear volume. In the case of HEP with two nucleoli (or more), the measurements were performed for the two (or more) particles (Gundersen, 1988).

Positive and negative controls (omission of first antibody and replacement by non-immune serum) were included, both in thin

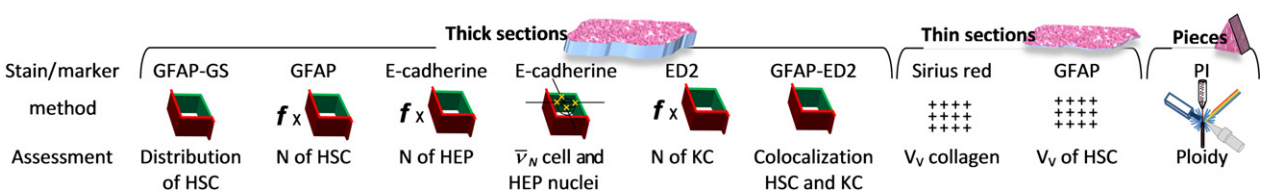

HEP: hepatocytes; HSC: hepatic stellate cells; KC: Kupffer cells; N: total number; V_V: relative volume, $\overline{v}_N$ number-weighted mean cell volume.

Figure 1 Overview of the methods used in this study in thin and thick liver sections and in frozen pieces.

and thick sections, and all slides were evaluated blindly (i.e. the observer was unaware of the sex of the animal) to avoid any observer-related bias.

Thin sections

Immunohistochemistry

A streptavidin–biotin protocol was also used (Histostain Plus) for glial fibrillary acidic protein immunostaining. In this case, shorter incubation times were needed: the antibody was diluted to 1 : 1200 and incubated overnight, and the blocking solution, secondary antibody and streptavidin–peroxidase complex were all applied for 20 min; colour development in DAB was restricted to 2 min.

Histochemical Sirius red staining

Thin sections were counterstained with Celestial blue and Mayer's haematoxylin, each for 5 min; then, after washing in tap water, the Sirius red (coloration index 35782; Sigma) dissolved in picric acid (1 mg mL^{-1}) was applied for 1 h at room temperature (Junqueira et al. 1978). After washing in acidified water (1% acetic acid), sections were dehydrated, cleared and mounted.

Stereological analysis

Five sections were randomly selected per animal and an average of 150 oil-immersion fields were quantified per animal (fields were 'selected' after systematic uniform random sampling performed by the software). A test-system of points was superimposed by the software to determine the relative volume of HSC in the slides immunostained against glial fibrillary acidic protein (Fig. 2). The test-system included 12 sparser points, used to quantify the reference space (whole liver), and 108 denser ones, used for HSC. The relative volume of HSC was estimated as the ratio of the two sets of points (Marcos et al. 2012). This parameter was multiplied by the liver volume and divided by the total number of HSC to estimate the number-weighted mean cell volume of HSC (Marcos et al. 2012).

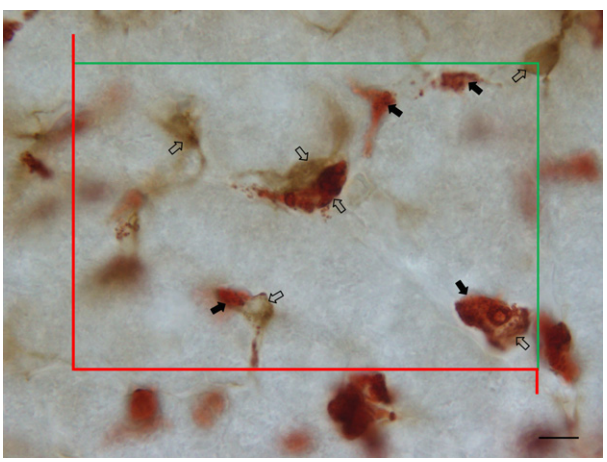

Figure 3 Thick liver section immune-stained against glial fibrillary acidic protein and ED2 for detecting hepatic stellate cells (HSC, black arrows) and Kupffer cells (KC, open arrows), respectively. Cells were counted if their nucleus was in focus below 4 μm and above or equal to 24 μm in the *z*-axis (section depth), if they were inside the inclusion (green) lines, or not touching the exclusion (red) lines. Scale bar: 6 μm.

The amount of collagen in Sirius red-stained slides was also evaluated by a similar strategy, but with 40× magnification lens (rendering a final magnification of 1600× at the screen) and a scanter test system of 36 points (which was judged adequate to estimate the relative volume of collagen). Point counting was used to determine the relative volume of fibrous tissue (collagen I and III) in the liver, focusing on three different locations: (1) Glisson's capsule; (2) vascular (portal spaces and around central veins); (3) intralobular (surrounding sinusoids).

Flow cytometry

To determine ploidy differences, liver pieces (≈ 0.7 g) frozen at −80 °C were gently thawed in phosphate-buffered saline (pH 7.4) and mechanically disaggregated with tweezers. The homogenate was centrifuged at 750 *g* for 5 min, and the supernatant decanted. The pellet was suspended in phosphate-buffered saline and the cell yield calculated in a haematology analyser (LH 780, Beckman Coulter, Brea, CA, USA). Afterwards, the suspension was split into two parts: one for cytological examination (cytospins) and the other for flow cytometry. For the latter, one 100-μL aliquot of each sample (with an average of 3×10^6 cells μL^{-1}) was stained using the Coulter DNA-Prep Reagents Kit (Beckman Coulter), according to the manufacturer's instructions. This was performed by sequentially dispensing and mixing 100 μL of the lysing and permeabilising reagent (DNA Prep LPR), and 1 mL of the staining solution containing 50 μg mL^{-1} propidium iodide and 4 kU mL^{-1} bovine pancreas type III RNAase (DNA Prep Stain). Finally, samples were incubated for 20 min in the dark. For the flow cytometry analysis, a Coulter EPICS-XL-MCL (Beckman Coulter) with a 488-nm argon ion laser was used. Sample acquisition was performed for a minimum of 30 min and a minimum of 20 000 events per sample were acquired. Rat lymphocytes were employed as a control for diploid cells. Analysis was performed with the MultiCycle software (Phoenix Flow Systems, San Diego, CA, USA), with modified exponential debris function. The percentage of diploid, tetraploid and octaploid particles was assessed.

Statistical analysis

The software SPSS 18 (IBM, Armonk, NY, USA) was used. After checking whether the data followed a normal distribution with the Shapiro–Wilk's test, a correlation analysis was conducted to detect linear correlations. Subsequent to assessing the homogeneity of variances (Levene's test), the Student's *t*-test for unpaired samples was used for comparing the means from males and females. In the case of liver weight, relative volume of collagen and variables related to HSC (total number, number per gram, number-weighted mean cell volume and lobular distribution), the non-parametric equivalent, the Mann–Whitney *U*-test, was used for comparing medians from males and females. Significance was set at $P \leq 0.05$.

Results

Livers displayed a normal morphology, without noticeable differences across animals. The livers of males were significantly heavier ($P = 0.02$) than those of females (14.11 ± 2.9 g vs. 9.75 ± 0.7 g, respectively). Likewise, male livers were significantly larger. The liver-to-body weight ratio was 4.0 ± 0.7 and 4.5 ± 0.6% in males and females, respectively. A very strong correlation was observed

between liver and body weight ($r = 0.8$; $P = 0.01$). Hepatic transaminase values were within the reference ranges (14–80 IU L^{-1} for alanine and 40–383 IU L^{-1} for aspartate transaminase levels), presenting no significant differences (42.0 ± 5.6 and 29.3 ± 10.9 IU L^{-1} for alanine and 98.8 ± 52.8 and 88.0 ± 42.2 IU L^{-1} for aspartate transaminase in males and females, respectively).

Thick sections

An average of 509 and 273 disectors were analysed for male and female rats, respectively. The total number of HSC was significantly higher in males than in females ($P = 0.016$) but their number per gram was similar (Table 1). By way of contrast, the total number of HEP was similar in males and females, although the latter had a significantly higher number per gram ($P = 0.016$). The same was seen for the BnHEP and KC: where the number per gram was significantly higher in females ($P = 0.016$), but the total number was similar in both sexes. The proportion of BnHEP was $24.8 \pm 4.2\%$ for males and $33.8 \pm 4.7\%$ for females, indicating no significant difference. It is noteworthy that the coefficient of error of the number estimations of HSC, HEP and KC was low, being between 0.039 and 0.060. This means that the methodological variability contributed much less to the total variance than did the biological component (the latter was responsible for 80–93% of the total variance).

A very strong correlation was observed between the total number of HSC and liver weight ($r = 0.85$, $P = 0.004$). In addition, the number per gram of HEP was also correlated with that of KC and with the number per gram of BnHEP ($r = 0.94$, $P < 0.001$ and $r = 0.75$, $P = 0.02$, respectively). The relative volume of intralobular collagen was correlated only with the total number of HEP ($r = 0.74$, $P = 0.037$) – this correlation was mainly with mononucleated HEP, as no correlation existed with the number of BnHEP. The percentage of BnHEP was negatively correlated with bodyweight ($r = -0.81$, $P = 0.015$) and with the total number of HEP ($r = -0.76$, $P = 0.028$).

The number-weighted mean cell and nuclear volume of HEP was also evaluated; on average, 107 HEP per animal were assessed for these purposes (Table 2). Male vs. female differences existed for mononucleated HEP ($P = 0.002$) but not for BnHEP. Mononucleated cells were 21–34% smaller than BnHEP ($P < 0.001$). Significant male/female differences existed in the number-weighted mean nuclear volume for mononucleated HEP ($P = 0.029$). The histogram of the number-weighted mean nuclear volume revealed small differences: young females exhibited a slightly skewed pattern (Pearson's skewness = 1.0; kurtosis = 3.38) compared with males (Pearson's skewness = 0.34; kurtosis = 0.51) (Fig. 4). Considering that the histogram featured two modes, observed in data from both females and males, we computed this as two distributions (one for diploid cells and the other for tetraploid cells). The first mode was considered the mean of the diploid cells and the second the mean of the tetraploid cells. The standard deviation for each group was calculated based on the means. In this way, we estimated the number-weighted mean nuclear volume of the diploid nuclei as 225 ± 36 μm^3, and of the tetraploid nuclei as 447 ± 52 μm^3. The number-weighted mean nuclear volumes of mononucleated HEP and BnHEP were not significantly correlated with their respective cell volumes ($P = 0.085$ and 0.072, respectively). In BnHEP, the two nuclei presented volumes of the same order of magnitude, but the coefficient of variance between nuclei varied by up to 14%. The nuclear to cytoplasm ratio was between 9.2 and 11.9%, and no differences existed between mononucleated and BnHEP.

To determine the distribution of HSC in liver lobules, we evaluated an average of 303 HSC per animal; cells were significantly more abundant in centrilobular regions ($56.5 \pm 4.5\%$) than in periportal locations ($43.3 \pm 4.3\%$) ($P = 0.001$). The distribution of cells was similar in males and females and no staining intensity differences could be detected between these locations. As to cells neighbouring HSC, we should stress that the thick sections, encompassing all KC and HSC cell processes, allowed easy recognition of cell juxtapositions (Fig. 3). On average, we evaluated 188 HSC per animal, noting that $41.6 \pm 6.7\%$ were physically positioned next to KC in males. In females a lower number of HSC ($26 \pm 7.4\%$) had KC for neighbours; the difference in the position of these two cells was statistically significant ($P = 0.001$).

Thin sections

An average of 216 fields were screened per animal. In males, the intralobular collagen corresponded to 56% of

Table 1 Estimations of the total number (N), number per gram (N g^{-1}) of hepatic stellate cells (HSC), hepatocytes (HEP) and Kupffer cells (KC) in 2 months male and female Wistar rats. The percentage of binucleated hepatocytes (BnHEP), as well as their N g^{-1} is also included.

Parameters	N HSC ($\times 10^6$)	N g^{-1} HSC ($\times 10^6$)	N HEP ($\times 10^6$)	N g^{-1} HEP ($\times 10^6$)	% BnHEP	N g^{-1} BnHEP ($\times 10^6$)	N KC ($\times 10^6$)	N g^{-1} KC ($\times 10^6$)
Males	208 ± 37*	14.0 ± 2.2	1948 ± 349	136 ± 11*	24.8 ± 4.2	30.3 ± 9.2*	284 ± 51	19.7 ± 2.8*
Females	127 ± 19*	13.5 ± 2.6	1734 ± 348	183 ± 39*	33.8 ± 4.7	60.5 ± 7.7*	285 ± 47	30.1 ± 6.0*

*Significant differences across gender (Mann–Whitney's *U*-test). Data expressed as mean ± standard deviation (SD).

Table 2 Estimation of the number-weighted mean volume ($\bar{v}_N$) of cells and nuclei of mononucleated hepatocytes (MnHEP) and binuclear hepatocytes (BnHEP) in male and female rats.

	Males		Females	
	$\bar{v}_N$ nuclei (μm^3)	$\bar{v}_N$ cell (μm^3)	$\bar{v}_N$ nuclei (μm^3)	$\bar{v}_N$ cell (μm^3)
MnHEP	554 ± 25*	6044 ± 381*	509 ± 19*	4789 ± 286*
BnHEP	330 ± 53	7530 ± 813	371 ± 27	6565 ± 285

Data expressed as mean ± SD. *Significant differences across gender.

the total collagen, whereas 20 and 14% were located in portal tracts and around central venules, respectively, and only 10% were found in the Glisson's capsule. A similar scenario existed in females: 46% were intralobular, 42% around vessels (respectively, 28 and 14% in a portal and central location) and 12% in the capsule. No significant differences existed in these proportions between males and females. No differences in the collagen content in the liver, existed between males (2.05 ± 0.2%) and females (1.95 ± 0.3%).

In thin paraffin sections we also evaluated the relative volume of HSC immunostained by glial fibrillary acidic protein (Fig. 2). No statistical differences existed for this parameter across the sexes (Table 1). No statistical differences were noted in the number-weighted mean cell volume of HSC: male and female HSC had volumes of 619 ± 128 and 786 ± 192 μm^3, respectively.

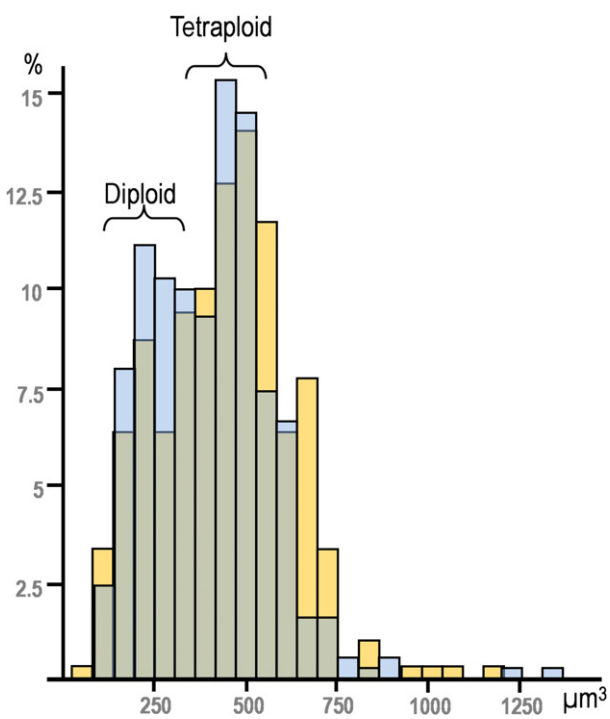

Figure 4 Histogram of the number-weighted mean nuclear volume of hepatocytes in males (yellow) and female (blue). The volume of diploid nuclei was estimated to be 225 ± 36 μm^3, whereas that of tetraploid nuclei was 447 ± 52 μm^3.

Flow cytometry

Owing to the mechanical dispersion of the liver cells and to the washing procedure, followed by slow speed centrifugation, non-hepatocytes were present in low numbers (an average of less than 5% of the nuclei), as verified by the liver rendering a mixture of particles, mostly formed by HEP nuclei (easily identified by their large size and presence of nucleoli) and well preserved HEP (both mononucleated by light microscopy, in the cytospin smears).

The flow cytometry analysis showed that the percentage of diploid particles (i.e. diploid naked nuclei mixed with diploid cells) tended to be more abundant in females (Table 3): significant differences existed between males and females ($P = 0.02$). No octaploid particles were observed.

Discussion

In this paper, we document, for the first time, the existence of linear correlations across liver cells. Apart from the strong correlation between the liver weight and the total number of HSC, these were also correlated with HEP; furthermore, correlations were established with BnHEP and KC. This emphasises the complex functional interplay that takes place in the liver, which will be discussed below, cell by cell.

Hepatic stellate cells

As liver fibrosis differs across sex in humans and rats, it could be hypothesised that baseline microanatomical differences in HSC exist in the normal organ. However, this was not supported by our data, as no quantitative differences were observed.

With regard to collagen deposition, a well recognised end-product of HSC (Friedman, 2008), no sexual differences exist and this is in accordance with previous studies that estimated collagen by hydroxyproline content (e.g. Shimizu et al. 1999). Our estimation of the relative volume of colla-

Table 3 Percentage of diploid and tetraploid particles in male and female rat liver estimated by flow cytometry.

	Males	Females
Diploid	84.9 ± 5.1*	92.9 ± 2.0*
Tetraploid	15.0 ± 5.1	7.1 ± 2.0

Data expressed as mean ± SD. *Significant differences across gender.

gen and its distribution in the liver are also in accordance with previous studies (Harkness & Harkness, 1954; Gascon-Barré et al. 1989). The synthesis of extracellular matrix and collagen in normal liver is ascribed to various cell types besides HSC, including HEP and liver sinusoidal endothelial cells (Friedman, 2008) but, surprisingly, of the three cell types examined here, we found a correlation only with HEP. This suggests that these cells may be the most relevant for collagen production in a normal setting, contrasting with cirrhotic livers, in which HSC have a leading role (Gressner & Weiskirchen, 2006).

The mean cellular volume of HSC has, to the best of our knowledge, never been reported. In this study, we opted for an indirect approach to estimate the number-weighted mean cell volume, because local estimators (for instance the nucleator) would be extremely difficult to implement. HSC have cellular extensions expanding in various directions (Oikawa et al. 2002) that would be in and out of focus in thick sections. It should be noted that our estimation ($\approx$ 700 μm^3 in males and females) is satisfactory for practical purposes but represents a slight underestimation because we highlighted the cytoskeleton and not the cell borders. Regarding volume estimation and HSC, the single study that estimated their relative volume obtained values of 0.4 $\pm$ 0.1% (Martin et al. 1992a), which is comparable to our figure of 0.3 $\pm$ 0.1%.

The lobulation of HSC has never been studied by stereology but has been a controversial topic. Herein, we reported a pericentral predominance in both males and females, but Wake (1980) and Geerts et al. (1991) – using vitamin autofluorescence and immunohistochemistry against desmin, respectively – reported a periportal predominance. Nevertheless, Higashi & Senoo (2003) and Senoo et al. (2007) used similar methods but found no lobular differences. The fact that we used antigen retrieval and long incubation times in paraffin sections (in contrast to the cryostat sections used in most studies) probably accounts for the differences. Moreover, a stereological strategy in thick sections should be more reliable for quantifying lobular heterogeneity, as thin sections viewed at low magnification are naturally biased towards periportal areas, which are far more cellular (Teutsch et al. 1999).

Hepatocytes

Sexual differences in HEP have never been evaluated by quantitative morphology, as far as we are aware. Regarding their total number, we did not observe significant male/female differences – even if they could be expected due to the geometric scaling related to a larger liver and body size of males. Surprisingly, sexual dimorphism was evident when assessing the number of HEP per gram, the so-called hepatocellularity. This parameter is important not only because it allows a straightforward comparison between studies, but also because it is widely used when *in vivo* hepatic clearance needs to be predicted (Barter et al. 2007). Using different methodologies, hepatocellularity in the male rat has ranged from 85 $\times$ 10^6 HEP g^{-1}(Carlile et al. 1997) to almost double that figure at 163 $\times$ 10^6 HEP g^{-1} (Smith et al. 2008); in humans, the value of 120 $\times$ 10^6 HEP g^{-1} has been predicted from the study of liver microsomes (Hirota et al. 2001). Sexual differences have rarely been considered, but Atchley et al. (2000) proposed their existence in mice (after puberty), with females having significantly more and smaller HEP than males; overall, this is in accordance with our data. The higher hepatocellularity in females may be explained by effects of oestrogens, as, at least *in vitro*, ethinylestradiol has induced a sevenfold increase in HEP proliferation, with DNA synthesis, but without cytotoxicity or induction of cytochrome-P-450 (Vickers & Lucier, 1996). A pioneer study by Fisher et al. (1984) also showed that the livers of female rats receiving multiple injections of oestradiol were 27% heavier and had an increased amount of total DNA.

We highlighted a negative correlation between BnHEP percentage and liver bodyweight. A negative correlation between binuclearity, nuclear ploidy and bodyweight seems to be a feature of mammals, including rats (Vinogradov et al. 2001). It has been known for more than 60 years (St Aubin & Bucher, 1952) that the percentage of BnHEP decreases while the total number of HEP increases during normal rat growth and in partial hepatectomy. This phenomenon is also suggested by our data, showing a negative correlation between the percentage of BnHEP and the total number of HEP. Even if no sexual differences existed in the percentage of BnHEP, we observed significant differences in their numbers per gram. This could be related to insulin, as *in vitro* studies have demonstrated that epidermal growth factor and insulin induced a high rate of BnHEP, similar to that normally observed in the liver of growing rats (Mossin et al. 1994). More recently, it was reported that rats with low insulin levels had less BnHEP formation compared with animals injected with the hormone (Celton-Morizur & Desdouets, 2010). Interestingly, differences in insulin also appear to exist in normal rats, with higher levels in females (Lopes da Costa et al. 2004; Vital et al. 2006). Oestrogens may also play a role here, as oophorectomised rats have significantly lower insulin levels that can be restored by oestradiol administration (Ahmadi & Oryan, 2008). The functional significance of sexual dimorphism in the number per gram of HEP and BnHEP is still unknown, but it may underlie the larger functional reserve and the higher regenerative potential reported for the female liver (Shimizu et al. 2007).

Another interesting finding of our study relates to the volume of HEP. It is often assumed that BnHEP are twice the size of mononucleated HEP (e.g. Celton-Morizur & Desdouets, 2010; Crawford & Burt, 2012). As a twofold increase in volume corresponds to only a 1.4-fold increase in surface area, this would result in less efficient transport in BnHEP

(Pandit et al. 2013). The twofold assumption has been substantiated by classical studies that dissociated HEP mechanically (Epstein, 1967; Martin et al. 1992b). It should be noted that isolated HEP tend to enlarge because they do not have compressive forces of adjacent cells and they often appear flattened (and further enlarged) below the coverslip (St Aubin & Bucher, 1952). Our data strongly contradict a twofold proportionality, because the number-weighted mean cell volume of BnHEP is only 25–37% larger than that of mononucleated HEP and no correlation existed between the mean volume of these cells. In fact, the use of different meshes to sort HEP after isolation has already shown that cell size is not correlated with binuclearity or ploidy (Gandillet et al. 2003).

It should be emphasised that the number-weighted mean cell volume of HEP is an important parameter in research, being considered the best predictor of liver cancer in rodents (Hall et al. 2012). Overall, our data on the volume of HEP coincides with reported figures (5000–6000 μm^3; McCuskey, 2006; Grisham, 2009) and closely resembles those of Jack et al. (1990), who also used stereological methods.

Kupffer cells

To the best of our knowledge, this is the first report of sexual dimorphism in the number per gram of KC. Notably it has been shown that female rats as well as mice have $\approx$ 50% more macrophages than males, both in their pleural and peritoneal cavities, with more Toll-like receptors and greater phagocytic efficiency (Scotland et al. 2011). Even if new numerical differences were disclosed herein, it has been known for a long time that KC are influenced by oestrogen: peaks of phagocytosis and proliferation have been correlated with elevated oestrogen in the oestrous cycle of mice and rats (Nicol & Veron-Roberts, 1965; Vickers & Lucier, 1996).

The HSC-KC proximity should favour the crosstalk and paracrine/juxtacrine stimulation among these cells, which nowadays is viewed as reciprocal (Tacke & Zimmermann, 2014). As liver sinusoids have fenestrae, it is easy for intrasinusoidal KC to contact perisinusoidal HSC directly. The relationship between these cells has a long history; it has been known for more than 25 years that the conditioned medium of KC is able to stimulate collagen synthesis and activation of HSC (Friedman & Arthur, 1989), whereas HSC-derived molecules promote the differentiation of a more pro-inflammatory and pro-fibrotic phenotype of KC (Chang et al. 2013). Because sexual differences exist in the constellation of HSC-KC – *viz.* 41.6 $\pm$ 6.7% and 26 $\pm$ 7.4% in males and females, respectively – it could be hypothesised that a less pro-inflammatory KC phenotype could be present in the female rat liver.

In conclusion, we have demonstrated that HEP and KC, but not HSC, have significant sexual dimorphism. This may be due to oestrogens acting in α-receptors, which functionally exist in HEP and KC but not in HSC (Shimizu et al. 2007). In view of the fact that mechanisms underlying clinically sexual dimorphism are largely unknown (Yokoyama et al. 2007; Li et al. 2012), this study adds substantial understanding by showing that primal morphological quantitative differences do exist in the rat liver. This should be taken into account when planning studies and interpreting sexual differences in liver regeneration, inflammatory and fibrotic conditions. It would be particularly interesting to investigate whether our findings in rats also apply to humans.

Acknowledgements

This work was financially supported by FEDER funds through the Competitiveness and Trade Expansion Program (COMPETE) and by national funds, Fundação para a Ciência e Tecnologia (FCT) via a doctoral grant (SFRH/BD/38958/2007). We are deeply grateful to Madelaine Henry for English language editing.

Conflict of interest

The authors declare that they have no conflict of interest.

References

Ahmadi R, Oryan Sh (2008) Effects of ovariectomy or orchidectomy and estradiol valerate or testosterone enanthate replacement on serum insulin in rats. *Pak J Biol Sci* **15**, 306–308.

Atchley WR, Wei R, Crenshaw P (2000) Cellular consequences in the brain and liver of age-specific selection for rate of development in mice. *Genetics* **155**, 1347–1357.

Barter ZE, Bayliss MK, Beaune PH, et al. (2007) Scaling factors for the extrapolation of *in vivo* metabolic drug clearance from *in vitro* data: researching a consensus on values of human microsomal protein and hepatocellularity per gram of liver. *Curr Drug Metab* **8**, 33–45.

Biondo-Simões ML, Matias JE, Montibeller GR, et al. (2006) Effect of aging on liver regeneration in rats. *Acta Cir Bras* **21**, 197–202.

Carlile DJ, Zomorodi K, Houston JB (1997) Scaling factors to relate drug metabolic clearance in hepatic microsomes, isolated hepatocytes, and the intact liver: studies with induced livers involving diazepam. *Drug Metab Dispos* **25**, 903–911.

Celton-Morizur S, Desdouets C (2010) Polyploidization of liver cells. *Adv Exp Med Biol* **676**, 123–135.

Chang J, Hisamatsu T, Shimamura K, et al. (2013) Activated hepatic stellate cells mediate the differentiation of macrophages. *Hepatol Res* **43**, 658–669.

Crawford JM, Burt AD (2012) Anatomy, pathophysiology and basic mechanisms of disease. In: *MacSween's Pathology of the Liver*. 6th edn (eds Burt A, Portmann B, Ferrell L), pp. 1–74, Edinburgh: Churchill Livingstone.

Croome KP, Segal D, Hernandez-Alejandro R, et al. (2014) Female donor to male recipient gender discordance results in inferior graft survival: a prospective study of 1,042 liver transplants. *J Hepatobiliary Pancreat Sci* **21**, 269–274.

Davidson AJ, Castañón-Cervantes O, Stephan FK (2004) Daily oscillations in liver function: diurnal vs circadian rhythmicity. *Liver Int* **24**, 179–186.

Dorph-Petersen KA, Nyengaard JR, Gundersen HJG (2001) Tissue shrinkage and unbiased stereological estimation of particle number and size. *J Microsc* **204**, 232–246.

Epstein CJ (1967) Cell size, nuclear content, and the development of polyploidy in the mammalian liver. *Proc Natl Acad Sci U S A* **57**, 327–334.

Fisher B, Gunduz N, Saffer EA, et al. (1984) Relation of estrogen and its receptor to rat liver growth and regulation. *Cancer Res* **44**, 2410–2415.

Friedman SL (2008) Hepatic stellate cells: protean, multifunctional, and enigmatic cells of the liver. *Physiol Rev* **88**, 125–172.

Friedman SL, Arthur MJ (1989) Activation of cultured rat hepatic lipocytes by Kupffer cell conditioned medium. Direct enhancement of matrix synthesis and stimulation of cell proliferation via induction of platelet-derived growth factor receptors. *J Clin Invest* **86**, 1780–1785.

Gandhi CR (2012) Augmenter of liver regeneration. *Fibrogenesis Tissue Repair* **5**, 10.

Gandillet A, Alexandre E, Holl V, et al. (2003) Hepatocyte ploidy in the normal rat. *Comp Biochem Physiol A Mol Integr Physiol* **134**, 665–673.

Gascon-Barré M, Huet PM, Belgiorno J, et al. (1989) Estimation of collagen content of liver specimens. Variation among animals and among hepatic lobes in cirrhotic rats. *J Histochem Cytochem* **37**, 377–381.

Gebhardt R, Mecke D (1983) Heterogeneous distribution of glutamine synthetase among rat liver parenchymal cells *in situ* and in primary culture. *EMBO J* **2**, 567–570.

Geerts A, Lazou JM, De Bleser P, et al. (1991) Tissue distribution, quantitation and proliferation kinetics of fat-storing cells in carbon tetrachloride-injured rat liver. *Hepatology* **13**, 1193–1202.

Grebely J, Page K, Sacks-Davis R, et al. (2014) The effects of female sex, viral genotype, and IL28 genotype on spontaneous clearance of acute hepatitis C virus infection. *Hepatology* **59**, 109–120.

Gressner AM, Weiskirchen R (2006) Modern pathogenetic concepts of liver fibrosis suggest stellate cells and TGF-beta as major players and therapeutic targets. *J Cell Mol Med* **10**, 76–99.

Grisham JW (2009) Organizational principles of the liver. In: *The Liver: Biology and Pathobiology*. 5th edn (eds Arias IM, Alter HJ, Boyer JL, Cohen DE, Fausto N, Shafritz DA, Wolkoff AW), pp. 3–15, New York: John Wiley & Sons Ltd.

Gundersen HJ (1988) The nucleator. *J Microsc* **151**, 3–21.

Gupta S (2000) Hepatic polyploidy and liver growth control. *Semin Cancer Biol* **10**, 161–171.

Hall AP, Elcombe CR, Foster JR (2012) Liver hypertrophy: a review of adaptative (adverse and non-adverse) changes – conclusions from the 3rd International ESTP Expert Workshop. *Toxicol Pathol* **40**, 971–994.

Harkness ML, Harkness RD (1954) Further observations on collagen in regenerating liver of the rat. *J Physiol* **123**, 482–491.

Higashi N, Senoo H (2003) Distribution of vitamin A-storing lipid droplets in hepatic stellate cells in liver lobules – a comparative study. *Anat Rec A Discov Mol Cell Evol Biol* **271**, 240–248.

Hirota N, Ito K, Iwatsubo T, et al. (2001) *In vitro/in vivo* scaling of alprazolam metabolism by CYP3A4 and CYP3A5 in humans. *Biopharm Drug Dispos* **22**, 53–71.

Imamura H, Shimada R, Kubota M, et al. (1999) Preoperative portal vein embolization: an audit of 84 patients. *Hepatology* **29**, 1099–1105.

Jack EM, Bentley P, Bieri F, et al. (1990) Increase in hepatocyte and nuclear volume and decrease in the population of binucleated cells in preneoplastic foci of rat liver: a stereological study using the nucleator method. *Hepatology* **11**, 286–297.

Junqueira LC, Cossermelli W, Brentani R (1978) Differential staining of collagens type I, II and III by Sirius Red and polarization microscopy. *Arch Histol Jpn* **41**, 267–274.

Kitagawa T, Yokoyama Y, Kokuryo T, et al. (2009) Estrogen promotes hepatic regeneration via activating serotonin signal. *Shock* **31**, 615–620.

Kmieć Z (2001) Cooperation of liver cells in health and disease. *Adv Anat Embryol Cell Biol* **161**, 1–151.

Lai JC, Feng S, Roberts JP, et al. (2011) Gender differences in liver donor quality are predictive of graft loss. *Am J Transplant* **11**, 296–302.

Li Z, Tuteja G, Schug J, et al. (2012) Foxa1 and Foxa2 are essential for sexual dimorphism in liver cancer. *Cell* **148**, 72–83.

Lopes Da Costa C, Sampaio de Freitas M, Sanchez Moura A (2004) Insulin secretion and GLUT-2 expression in undernourished neonate rats. *J Nutr Biochem* **15**, 236–241.

Marcos R, Monteiro RA, Rocha E (2004) Estimation of the number of stellate cells in a liver with the smooth fractionator. *J Microsc* **215**, 174–182.

Marcos R, Monteiro RAF, Rocha E (2006) Design-based stereological estimation of hepatocyte number, by combining the smooth optical fractionator and immunocytochemistry with anticarcinoembryonic antigen polyclonal antibodies. *Liver Int* **26**, 116–124.

Marcos R, Monteiro RAF, Rocha E (2012) The use of design based stereology to evaluate volumes and numbers in the liver: a review with practical guidelines. *J Anat* **220**, 303–317.

Martin G, Sewell RB, Yeomans ND, et al. (1992a) Ageing has no effect on the volume density of hepatocytes, reticuloendothelial cells or the extracellular space in livers of female Sprague-Dawley rats. *Clin Exp Pharmacol Physiol* **19**, 537–539.

Martin NC, McCullough CT, Bush PG, et al. (1992b) Functional analysis of mouse hepatocytes differing in DNA content: volume, receptor expression and effect of INNγ. *J Cell Physiol* **191**, 138–144.

Massard J, Ratziu V, Thabut D, et al. (2006) Natural history and predictors of disease severity in chronic hepatitis C. *J Hepatol* **44**, S19–S24.

McCuskey RS (2006) Anatomy of the liver. In: *Zakim and Boyer's Hepatology. A Textbook of Liver Disease*, 5th edn,(eds Boyer TD, Wright TL, Manns MP), pp. 3–21, Philadelphia: Saunders.

Mossin L, Blankson H, Huitfeldt H, et al. (1994) Ploidy-dependent growth and binucleation in cultured rat hepatocytes. *Exp Cell Res* **214**, 551–560.

Nicol T, Veron-Roberts B (1965) The influence of the estrus cycle, pregnancy and ovariectomy on RES activity. *J Reticuloendothel Soc* **60**, 15–29.

Oikawa H, Masuda T, Kamaguchi J, et al. (2002) Three-dimensional examination of hepatic stellate cells in rat liver and response to endothelin-1 using confocal laser scanning microscopy. *J Gastroenterol Hepatol* **17**, 861–872.

Pandit SK, Westendorp B, Bruin A (2013) Physiological significance of polyploidization in mammalian cells. *Trends Cell Biol* **23**, 556–566.

Poynard T, Ratziu V, Charlotte F, et al. (2001) Rates and risk factors of liver fibrosis progression in patients with chronic hepatitis C. *J Hepatol* **34**, 730–739.

Santos M, Marcos R, Santos N, et al. (2009) An unbiased stereological study on subpopulations of rat liver macrophages and on their numerical relation with the hepatocytes and stellate cells. *J Anat* **214**, 744–751.

Scheicher J, Tokarski C, Marbach E, et al. (2015) Zonation of hepatic fatty acid metabolism – The diversity of its regulation and the benefit of modeling. *Biochim Biophys Acta* **1851**, 641–656.

Scotland RS, Stables MJ, Madalli S, et al. (2011) Sex differences in resident immune cell phenotype underlie more efficient acute inflammatory responses in female mice. *Blood* **118**, 5918–5927.

Senoo H, Kojima N, Sato M (2007) Vitamin A-storing cells (stellate cells). *Vitam Hormon* **75**, 131–159.

Shimizu I, Mizobuchi Y, Yasuda M, et al. (1999) Inhibitory effect of oestradiol on activation of rat hepatic stellate cells *in vivo* and *in vitro*. *Gut* **44**, 127–136.

Shimizu I, Kohno N, Tamaki K, et al. (2007) Female hepatology: favorable role of estrogen in chronic liver disease with hepatitis B virus infection. *World J Gastroenterol* **13**, 4295–4305.

Sirma H, Williams GM, Gebhardt R (1996) Strain- and sex-specific variations in hepatic glutamine synthetase activity and distribution in rats and mice. *Liver* **16**, 166–173.

Smith R, Jones RD, Ballard PG, et al. (2008) Determination of microsome and hepatocyte scaling factors for *in vitro*/*in vivo* extrapolation in the rat and dog. *Xenobiotica* **38**, 1386–1398.

St Aubin PM, Bucher NL (1952) A study of binucleate cell counts in resting and regenerating rat liver employing a mechanical method for the separation of liver cells. *Anat Rec* **112**, 797–809.

Tacke F, Zimmermann HW (2014) Macrophage heterogeneity in liver injury and fibrosis. *J Hepatol* **60**, 1090–1096.

Teutsch HF (1984) Sex-specific regionality of liver metabolism during starvation; with special reference to the heterogeneity of the lobular periphery. *Histochemistry* **81**, 87–92.

Teutsch HF, Schuerfeld D, Groezinger E (1999) Three-dimensional reconstruction of parenchymal units in the liver of the rat. *Hepatology* **29**, 494–505.

Tsukamoto I, Kojo S (1990) The sex difference in the regulation of liver regeneration after partial hepatectomy in the rat. *Biochim Biophys Acta* **1033**, 287–290.

Vickers AE, Lucier GW (1996) Estrogen receptor levels and occupancy in hepatic sinusoidal endothelial and Kupffer cells are enhanced by initiation with diethylnitrosamine and promotion with 17 alpha-ethinylestradiol in rats. *Carcinogenesis* **17**, 1235–1242.

Villa E (2008) Role of estrogen in liver cancer. *Womens Health* **4**, 41–50.

Vinogradov AE, Anatskaya OV, Kudryavtsev BN (2001) Relationship of hepatocyte ploidy levels with body size and growth rate in mammals. *Genome* **44**, 350–360.

Vital P, Larrieta E, Hiriart M (2006) Sexual dimorphism in insulin sensitivity and susceptibility to develop diabetes in rats. *J Endocrinol* **190**, 425–432.

Wake K (1980) Perisinusoidal stellate cells (fat-storing cells, interstitial cells, lipocytes), their related structure in and around the liver sinusoids, and vitamin A-storing cells in extrahepatic organs. *Int Rev Cytol* **66**, 303–353.

Yang K, Du C, Cheng Y, et al. (2013) Augmenter of liver regeneration promotes hepatic regeneration depending on the integrity of Kupffer cell in rat small-for-size liver transplantation. *J Surg Res* **183**, 922–928.

Yasuda M, Shimizu I, Shiba M, et al. (1999) Suppressive effects of estradiol on dimethylnitrosamine-induced fibrosis of the liver in rats. *Hepatology* **29**, 719–727.

Yokoyama Y, Nagino M, Nimura Y (2007) Which gender is better positioned in the process of liver surgery? Male or female? *Surg Today* **37**, 823–830.